Influence of the singular manifold of non observable states in reconstructing chaotic attractors

Madalin Frunzete[1], Jean-Pierre Barbot[1,3] & Christophe Letellier [2]
[1] *Electronique et Commande des Systèmes Laboratoire, EA 3649 (ECS-Lab/ENSEA), Cergy-Pontoise, France*
[2] *CORIA UMR 6614, Université de Rouen, B.P. 12, F-76801 Saint-Etienne du Rouvray cedex, France and*
[3] *EPI Non-A, INRIA Lille Nord Europe*
(Dated: November 11, 2012, Partial draft of the paper *Physical Review E 86 (2012)*)

It is known that the reconstructed phase portrait of a given system strongly depends on the choice of the observable. In particular, the ability to obtain a global model from a time series strongly depends on the observability provided by the measured variable. Such a dependency results from i) the existence of a singular observability manifold $\mathcal{M}_s^{\rm obs}$ for which the coordinate transformation between $\mathbb{R}^m$ and the reconstructed space is not defined and ii) how often the trajectory visits the neighborhood $\mathcal{U}_{\mathcal{M}_s^{\rm obs}}$ of $\mathcal{M}_s^{\rm obs}$. In order to clarify how these aspects contribute to the observability coefficients, we introduce the probability of visits of $\mathcal{M}_s^{\rm obs}$ and the relative time spent in $\mathcal{U}_{\mathcal{M}_s^{\rm obs}}$ to construct a new coefficient. Combined with the symbolic observability coefficients previously introduced [Letellier & Aguirre, PRE, **79**, 066210, 2009] (only taking into account the existence of $\mathcal{M}_s^{\rm obs}$), this new coefficient helps to determine the specific role played by the location of $\mathcal{M}_s^{\rm obs}$ with respect to the attractor, in phase portrait reconstruction and in any analysis technique.

I. INTRODUCTION

Since Takens proved that from a single scalar time series it is possible to reconstruct a phase portrait which is diffeomorphically equivalent to the original portrait [1], the reconstruction procedure became the first step in dynamical analysis of chaotic behaviors. What is suggested by the Takens theorem is that, no matter of the variable chosen to reconstruct the phase portrait, a good enough reconstructed attractor is always obtained, provided a large enough number of coordinates is used. It was also shown by Aeyels that observability is a generic property for nonlinear systems [2]. Nevertheless, when a global modelling procedure is applied to a reconstructed chaotic attractor, that is, when a set of differential or difference equations reproducing the dynamics underlying a time series is directly estimated from that time series, a strong dependence of the quality of such global models on the "measured" variable is observed [3]. Such a result triggered some works to justify the observed departures. First based on a linear theory [4, 5] and then on a nonlinear theory [6], numerical observability coefficients were introduced to rank the different variables according to the observability of dynamics underlying the system investigated. This was shown to be useful for interpreting results of dynamical analysis, global modelling, control technique, etc. [7].

The numerical observability coefficients — averaged along a chaotic trajectory — take into account the structural component inherited from the algebraic structure of the equations and the dynamical component, that is, how often is visited the domains of the phase space where the observability is lost. This last component is rather important because the observability of nonlinear systems depends on the location in phase space. They thus provide a global quantification, in the unit interval, of the observability of the attractor through a given time series. Symbolic observability coefficients estimated from a fluence graph of the system were also introduced for quadratic systems [8]. These latter coefficients were only based on the algebraic structure of the system and, consequently, only consider the structural component to the observability problem: the relative organization of the singular observability manifold $\mathcal{M}_s^{\rm obs}$ — here defined as the singular set of points of the original state space which are not observable in the reconstructed space — and of the visited attractor was not considered by these latter coefficients. In particular, they do not take into account whether the attractor intersects the singular observability manifold $\mathcal{M}_s^{\rm obs}$ or not. Such a lack limits a little bit the interest of the symbolic observability coefficients in the sense that one can question the way according which the reconstruction process is affected by a lack of observability due to a singular observability manifold quite far from the attractor. In order to address this problem, we here introduce two measures (within the unit interval), namely the probability of visits and the relative time spent in a neighborhood of the singular observability manifold $\mathcal{M}_s^{\rm obs}$. From these two measures a new coefficient is constructed to interpret the role of the dynamical regime *via* the location of the attractor with respect to the singular observability manifold.

After a brief review about the observability coefficients in Section II, the probability of visits of the singular observability manifold, the relative time spent in it and the manifold observability coefficient, all of them introduced in Section III, are computed for each variable of the Rössler system and the Lorenz system. Some results obtained when two Rössler systems are bidirectionally coupled are explained in Section IV using these coefficients. Section V gives a conclusion.

II. OBSERVABILITY COEFFICIENTS

Let us consider the autonomous dynamical system

$$\begin{cases} \dot{\boldsymbol{x}} = \boldsymbol{f}(\boldsymbol{x}) \\ s = h(\boldsymbol{x}) \end{cases} \tag{1}$$

where $\boldsymbol{x} \in \mathbb{R}^m$ is the state vector and $h : \mathbb{R}^m \to \mathbb{R}$ the measurement function. The state space is therefore here assumed to be m-dimensional. When a phase portrait is reconstructed from a time series, it is commonly believed that, according to the Takens theorem [1], a diffeomorphim between the original space $\mathbb{R}^m(\boldsymbol{x})$ and the reconstructed space $\mathbb{R}^d(\boldsymbol{X})$ can be obtained provided d is large enough. One of the assumptions required by the Takens theorem is that the measurement function h must be generic, a condition not necessarily verified. In practice h is commonly not generic when h only returns one of the system variables. For instance, it has been remarked for a long time that when the Lorenz attractor is reconstructed from variable z, a global diffeomorphism cannot be obtained because the rotation symmetry is lost [9]. In the case of variable x or y, the symmetry of the reconstructed attractor is an inversion, and no longer a rotation. As a consequence, none of the three variables corresponds to a generic measurement function. It is thus not guaranteed that a global diffeomorphism exists between the original phase space and the differential embedding induced by the "measured" variable.

A way to take into account the lack of genericity of h is to consider the observability provided by the "measured" variable s. A possible definition for the observability of an autonomous system is as follows [10].

Definition 1 *An autonomous dynamical system (1) is said to be state observable at time t_f if every initial state $\boldsymbol{x}(0)$ can be uniquely determined from knowledge of a finite time history of the output $s(\tau)$, $0 \leq \tau \leq t_f$.*

One way of testing whether the system (1) is observable is to define and verify the rank of the *observability matrix* [11]

$$\mathcal{O} = \begin{bmatrix} \mathrm{d}h(\boldsymbol{x}) \\ \mathrm{d}\mathcal{L}_f h(\boldsymbol{x}) \\ \vdots \\ \mathrm{d}\mathcal{L}_f^j h(\boldsymbol{x}) \end{bmatrix} \tag{2}$$

where $\mathcal{L}^k$ is the kth order Lie derivative, with $j \geq m-1$. The Lie derivative of the ith component of the vector field $\boldsymbol{f}$ is defined as

$$\mathcal{L}_{f_i}(\boldsymbol{x}) = \sum_{k=1}^{m} f_k \frac{\partial f_i(\boldsymbol{x})}{\partial x_k} \,. \tag{3}$$

Higher-order derivatives are given recursively according to

$$\mathcal{L}_{f_j}^n(\boldsymbol{x}) = \mathcal{L}_{f_i}\left(\mathcal{L}_{f_i}^{n-1}(\boldsymbol{x})\right) \,. \tag{4}$$

Theorem 1 *Dynamical system (1) is state observable if and only if, $\exists j \geq m-1$ such that the matrix $\mathcal{O}_s \in \mathbb{R}^{j \times m}$ is full (column) rank, that is,* $\mathrm{rank}(\mathcal{O}_s) = m$ *[13].*

Remark 1 *Observable here should be understood as locally-weakly observable, in contrast to linear system the concept of observable is rarely global for nonlinear systems [12].*

Corollary 1 *Dynamical system (1) is state observable if and only if the $m \times m$ dimensional matrix $\mathcal{O}_s^T \mathcal{O}_s$ is non singular.*

For the sake of simplicity, we will limit ourselves to consider the regular local observability matrix $\mathcal{O}_s$, that is, to the case where $j = m-1$ [13].

Remark 2 *If the measurement function is defined by an identity matrix (i.e. all variables are measured), the dynamics is completely observable. The case where more than one variable (but not all) are measured is more difficult to treat [14]. In fact, the key point is to know what measurement functions should be preferred in term of Lie derivatives. Unfortunately, this is strongly system dependent [15–17]. When a single variable is measured, the measurement vector becomes a row vector and is directly responsible for any decrease in observability.*

It was shown [6] that the observability matrix $\mathcal{O}_s$ of a nonlinear system observed using variable s is exactly the Jacobian matrix $\mathcal{J}_{\Phi_s}$ of the map $\Phi_s : \mathbb{R}^m(\boldsymbol{x}) \to \mathbb{R}^m(\boldsymbol{X})$ between the original phase space $\mathbb{R}^m(\boldsymbol{x})$ and the reconstructed space $\mathbb{R}^m(\boldsymbol{X})$ where

$$\boldsymbol{X} = \begin{vmatrix} h(\boldsymbol{x}) \\ \mathcal{L}_f h(\boldsymbol{x}) \\ \vdots \\ \mathcal{L}_f^{m-1} h(\boldsymbol{x}) \,. \end{vmatrix} \tag{5}$$

The system is thus fully observable when the determinant $\mathrm{Det}\ \mathcal{J}_{\Phi_s}$ never vanishes, that is, when map Φ_s defines a global diffeomorphism (Φ_s musts be also one-to-one, a property observed in most of the cases). It is thus said that the system is "observable" if

$$\mathrm{rank}\ (\mathcal{O}_s) = m \Leftrightarrow\ \det\ (\mathcal{O}_s) \neq 0 \,. \tag{6}$$

The quality of an observable thus depends on the existence of a singular set defined by $\mathrm{Det}(\mathcal{J}_{\Phi_s}) = 0$, its dimension and its location with respect to the attractor. It is hence helpful to speak in terms of a *degree of observability* rather than in terms of a yes-or-no answer, that is, being observable or not.

Let us define the singular observability manifold $\mathcal{M}_s^{\mathrm{obs}}$ as

$$\mathcal{M}_s^{\mathrm{obs}} = \{\boldsymbol{x} \in \mathbb{R}^m \mid\ \det(\mathcal{O}(\boldsymbol{x})) = 0\} \,, \tag{7}$$

that is, as the domain of the state space $\mathbb{R}^m$ where the regular local observability is lost when measurements s

are used. Since it has been shown [6] that the observability matrix $\mathcal{O}_s(\boldsymbol{x})$ corresponds to the jacobian $\mathcal{J}_{\Phi_s}$ of the coordinate transformation Φ_s between the original space $\mathbb{R}^m(\boldsymbol{x})$ and the reconstructed space $\mathbb{R}^m(\boldsymbol{X})$, the singular observability manifold therefore represents the set of points of the original phase space $\mathbb{R}^m(\boldsymbol{x})$ which cannot be observed in the reconstructed space $\mathbb{R}^m(\boldsymbol{X})$. Consequently, it is important to know whether the attractor $\mathcal{A} \subset \mathbb{R}^m(\boldsymbol{x})$ intersects the singular observability manifold $\mathcal{M}_s^{\rm obs}$, since only such manifold will not be observable (reconstructed) in $\mathbb{R}^m(\boldsymbol{X})$.

As detailed in previous works (see [5, 6] among others), it is possible to compute an observability coefficient at each point of the phase space and for each observable. Since depending on the map Φ_s which is not too sensitive to parameter changes, the observability properties usually do not depend strongly on the dynamical regime. In fact, the observability as defined in corollary 1 does not depend on the dynamics but rather on the algebraic structure of the couplings between the different variables. In the case of quadratic systems, it was therefore possible to introduce a simple procedure to compute symbolic observability coefficients from the Jacobian matrix of the system under study. The algorithmic procedure to compute these symbolic observability coefficients is detailed in [18]. For instance, in the example of the Rössler system [19]

$$\begin{cases} \dot{x} = -y - z \\ \dot{y} = x + ay \\ \dot{z} = b + z(x - c)\,, \end{cases} \tag{8}$$

the symbolic observability coefficient are $\eta_x^{\rm R} = 0.92$, $\eta_y^{\rm R} = 1.00$, and $\eta_z^{\rm R} = 0.44$. In the case of the Lorenz system [20]

$$\begin{cases} \dot{x} = \sigma(y - x) \\ \dot{y} = Rx + y - xz \\ \dot{x} = -bz + xy\,, \end{cases} \tag{9}$$

the symbolic observability coefficients were found to be $\eta_x^{\rm L} = 0.89$, $\eta_y^{\rm L} = 0.29$, and $\eta_z^{\rm L} = 0.40$. How these departures in the observability coefficients may affect the analysis from a time series is discussed in [7, 18].

The standard definition of observability is a "yes" or "no" measure, that is, this definition only considers whether there is a singular observability manifold or not, as pointed out in [4]. The symbolic coefficients are more powerful because they rank the algebraic complexity of the singular observability manifold, but they do not take into account the location of the singular observability manifold with respect to the attractor. In practice, however, a system may gradually become unobservable as a parameter is varied. Moreover, for nonlinear systems, there are regions in state space that are less observable than others. The degree of observability was thus estimated using "numerical" observability coefficients defined as [5]

$$\delta(\boldsymbol{x}) = \frac{\mid \lambda_{\min}[\mathcal{O}_s^T\mathcal{O}_s, \boldsymbol{x}(t)] \mid}{\mid \lambda_{\max}[\mathcal{O}_s^T\mathcal{O}_s, \boldsymbol{x}(t)] \mid}, \tag{10}$$

where $\lambda_{\max}[\mathcal{O}_s^T\mathcal{O}_s, \boldsymbol{x}(t)]$ indicates the maximum eigenvalue of matrix $\mathcal{O}_s^T\mathcal{O}_s$ estimated at point $\boldsymbol{x}(t)$ (likewise for $\lambda_{\min}$) and $(\cdot)^T$ indicates the transpose. Then $0 \leq \delta(\boldsymbol{x}) \leq 1$, and the lower bound is reached when the system is unobservable at point $\boldsymbol{x}$. The "numerical" observability coefficients were calculated along a trajectory embedded (over a time duration T) in the attractor and the time averaged coefficient

$$\underline{\delta} = \frac{1}{T}\sum_{t=0}^{T} \delta\boldsymbol{x}(t) \tag{11}$$

were used.

The great advantage of these observability coefficients is that they take into account the algebraic structure of the dynamical system as well as the relative organization of the attractor and the singular observability manifold. Unfortunately, they are not normalized, forbidding to compare variables measured in different systems. Such a weakness motivated the introduction of the symoblic observability coefficients. To have at our disposal normalized coefficients taking into account the relative organization between the attractor $\mathcal{A}$ and $\mathcal{M}_s^{\rm obs}$, we thus introduce now two measures to adjoint to the symbolic observability coefficients.

III. INFLUENCE OF THE SINGULAR OBSERVABILITY MANIFOLD

A. Some definitions

The symbolic observability coefficients do not take into account the location of the observability manifold $\mathcal{M}_s^{\rm obs}$ with respect to the attractor $\mathcal{A} \subset \mathbb{R}^m(\boldsymbol{x})$. The objective is here to define a neighborhood $\mathcal{U}_{\mathcal{M}_s^{\rm obs}}$ of $\mathcal{M}_s^{\rm obs}$ and to estimate the probability $P_{\mathcal{M}_s^{\rm obs}}$ with which the trajectory visits $\mathcal{U}_{\mathcal{M}_s^{\rm obs}}$. The neighborhood can be defined as

$$\mathcal{U}_{\mathcal{M}_s^{\rm obs}} = \left\{(x, y, z) \in \mathbb{R}^3 \mid |\text{Det } \mathcal{J}_{\Phi_s}| < \epsilon\right\} \tag{12}$$

where

$$\epsilon = \mu\,[\text{ Max } (\text{Det } \mathcal{J}_{\Phi_s}) - \text{ Min } (\text{Det } \mathcal{J}_{\Phi_s})] \tag{13}$$

with $\mu = 0.05$. This latter value is quite arbitrary and we will check that our results are not too dependent on it. Let $P_{\mathcal{M}_s^{\rm obs}}$ be the probability for a trajectory $\{\boldsymbol{x}_n\}_{n=0}^N$ of measured points to be in the neighborhood $\mathcal{U}_{\mathcal{M}_s^{\rm obs}}$ of the singular observability manifold $\mathcal{M}_s^{\rm obs}$, that is, the probability for a point of the attractor $\mathcal{A}$ to be associated with

$$|\text{ Det } \mathcal{J}_{\Phi_s}| < \epsilon\,. \tag{14}$$

When the probability to have points $\boldsymbol{x} \in \mathcal{A} \bigcap \mathcal{M}_s^{\text{obs}}$ increases the number of points for which the original dynamics is not observable increases. We thus consider that the ability of the reconstructed attractor to provide a safe representation of the original phase portrait decreases. From that point of view, the ability to distinguish different states of the system in the reconstructed attractor decreases and $P_{\mathcal{M}_s^{\text{obs}}}$ can be considered as a measure of that ability. This probability not only takes into account the geometry of the attractor $\mathcal{A}$ with respect to the singular observability manifold $\mathcal{M}_s^{\text{obs}}$ but also the dynamics with which the attractor is visited since the "measured" points are distributed over the attractor with respect to the vector field. In other words, the measured points are not uniformely (geometrically speaking) distributed over the attractor.

A second ingredient important to estimate the impact the lack of observability may have on our ability to safely reconstruct a phase portrait from some measurements s is the time spent in the neighborhood of the singular observability manifold $\mathcal{U}_{\mathcal{M}_s^{\text{obs}}}$. Indeed, a long time interval spent in such a neighborhood will be more difficult to manage than a short time interval. In control system theory, it is well known that it is more difficult to observe a system spending quite rare long time duration in the neighborhood of $\mathcal{M}_s^{\text{obs}}$ than a system spending more frequent short time intervals in $\mathcal{U}_{\mathcal{M}_s^{\text{obs}}}$. This is due to the fact that for long time interval spent in $\mathcal{U}_{\mathcal{M}_s^{\text{obs}}}$ the observer must be transformed into an estimator (when the system is non observable, a model of that system must be used [21]). Such estimators are known to be quite sensitive to the model approximation, mainly because there is no term to correct the estimations (see [22] for an experimental example).

In order to evaluate damages actually caused by the singular observability manifold, we introduce the relative time $T_{\mathcal{M}_s^{\text{obs}}}$ with which the trajectory remains during a time $\tilde{T}_{\mathcal{M}_s^{\text{obs}}}$ in the neighborhood $\mathcal{U}_{\mathcal{M}_s^{\text{obs}}}$ divided by the pseudo-period T_0 of the system (the mean time interval between two consecutive intersections with a Poincaré section). We have thus

$$T_{\mathcal{M}_s^{\text{obs}}} = \frac{\tilde{T}_{\mathcal{M}_s^{\text{obs}}}}{T_0} \,. \tag{15}$$

Such a period can vary from one revolution to the other — this is particularly true for phase non-coherent attractor [23] — and, consequently, the mean value $\overline{T}_{\mathcal{M}_s^{\text{obs}}}$ will be used. A coefficient taking into account the way the singular observability manifold $\mathcal{M}_s^{\text{obs}}$ is visited is thus defined according to

$$\eta_s^{\text{obs}} = \left(1 - \overline{T}_{\mathcal{M}_s^{\text{obs}}}\right)\left(1 - P_{\mathcal{M}_s^{\text{obs}}}\right) \,. \tag{16}$$

This coefficient is designed as the manifold observability coefficients.

The most convenient situation is when $\eta_s^{\text{obs}} = 1$, that is, when the singular observability manifold is never visited by the trajectory ($P_{\mathcal{M}_s^{\text{obs}}} = 0$ and $\overline{T}_{\mathcal{M}_s^{\text{obs}}} = 0$). The worse situation is obviously when a fixed point x_* belongs to $\mathcal{M}_s^{\text{obs}}$ — typically this rarely occurs — or when the smallest velocity $\boldsymbol{v}(\boldsymbol{x})|_{\boldsymbol{x} \in \mathcal{M}_s^{\text{obs}}}$ is nearly zero: in the latter case, $\mathcal{A} \cap \mathcal{M}_s^{\text{obs}}$ can be rather small compared to attractor $\mathcal{A}$, but the time the trajectory spents in $\mathcal{U}_{\mathcal{M}_s^{\text{obs}}}$ is relatively large ($\overline{T}_{\mathcal{M}_s^{\text{obs}}} \approx 1$) and, consequently, the dynamics is not observable for significant parts of time, a condition sufficient to damage any analysis of the underlying dynamics.

B. Case of the Rössler system

In order to investigate the influence of the singular observability manifolds $\mathcal{M}_s^{\text{obs}}$ while reconstructing the Rössler attractor $\mathcal{A}$ from a time series s, let us start with the determinants of the jacobian matrix $\mathcal{J}_{\Phi_s}$ which are

$$\begin{cases} \text{Det } \mathcal{J}_{\Phi_x} = x - (a + c) \\ \text{Det } \mathcal{J}_{\Phi_y} = 1 \\ \text{Det } \mathcal{J}_{\Phi_z} = -z^2 \,, \end{cases} \tag{17}$$

respectively. It was shown [5] that the order of the singularity was correlated to the influence of $\mathcal{M}_s^{\text{obs}}$ in the reconstruction procedure. Roughly, higher the order of the singularity is, more influent the lack of observability is. This aspect is taken into account by the symbolic observability coefficients. There is therefore no need to consider this aspect in our two new measures. The singular observability manifolds corresponding to the three variables of the Rössler system are

$$\begin{cases} \mathcal{M}_x^{\text{obs}} = \{(x, y, z) \in \mathbb{R}^3 \mid x = a + c\} \\ \mathcal{M}_y^{\text{obs}} = \emptyset \\ \mathcal{M}_z^{\text{obs}} = \{(x, y, z) \in \mathbb{R}^3 \mid z = 0\} \,, \end{cases} \tag{18}$$

respectively. Since the determinant of the jacobian matrix $\mathcal{J}_{\Phi_y}$ never vanishes the corresponding singular observability manifold is an empty set. The two others correspond to planes in the state space as shown in Figs. 1. When the Rössler attractor is investigated *via* variable x, the singular observability manifold is a plane nearly perpendicular to the attractor flow: the mean relative time $\overline{T}_{\mathcal{M}_x^{\text{obs}}}$ spent in the neighborhood $\mathcal{U}_{\mathcal{M}_x^{\text{obs}}}$ is 0.08 s (Fig. 2a), and the influence of $\mathcal{M}_x^{\text{obs}}$ is rather weak.

The case where the Rössler attractor is observed *via* variable z is more interesting. There is no intersection between the Rössler attractor and the singular observability manifold $\mathcal{M}_z^{\text{obs}}$. Rigorously, this manifold has no impact on the reconstruction procedure of the Rössler attractor. But in practice, it is known [5–7] that variable z induces many difficulties to investigate the Rössler dynamics. For such a reason it is necessary to consider an influence domain of the singular observability manifold by considering all points in the neighborhood $\mathcal{U}_{\mathcal{M}_z^{\text{obs}}}$ defined according to Eq. (12). The probability density functions of

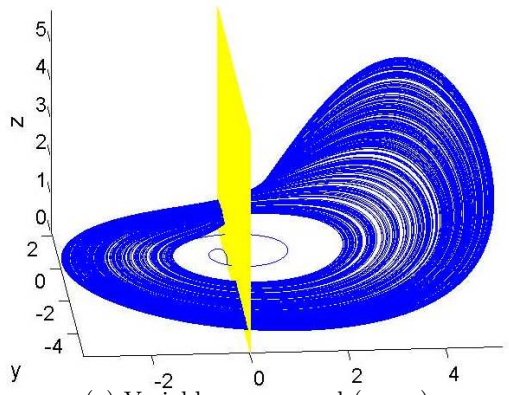

(a) Variable x measured ($s = x$)

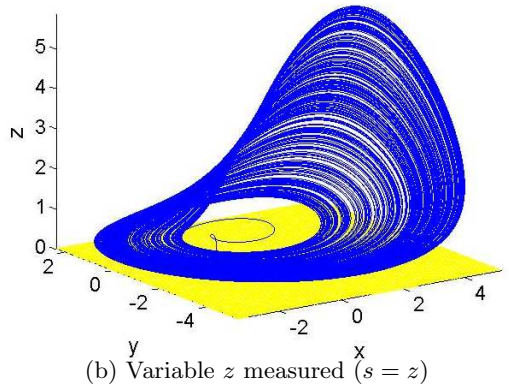

(b) Variable z measured ($s = z$)

FIG. 1: Chaotic attractor solution to the Rössler system (8) shown with the singular observability manifold in the cases where $s = x$ (a) and $s = z$ (b). Parameter values: $a = 0.398$, $b = 2$ and $c = 4$.

Det $\mathcal{J}_{\Phi_s}$ for the variables x and z of the Rössler system are shown in Fig. 2. The relative time $T_{\mathcal{M}_z^{\rm obs}}$ spent in the neighborhood $\mathcal{U}_{\mathcal{M}_x^{\rm obs}}$ can be quite large (Fig. 3b), since sometimes the trajectory spent almost $\frac{7}{4}T_0$ in it. Clearly, there are significant parts of the trajectory during which the dynamics is not seen by variable z and this would deeply affect any analysis applied to this variable.

The manifold observability coefficient $\mathcal{M}_x^{\rm obs}$ is thus rather large (Fig. 2a) with $\eta_x^{\mathcal{M}} = 0.86$ ($P_{\mathcal{M}_x^{\rm obs}} = 0.07$ and $\overline{T}_{\mathcal{M}_x^{\rm obs}} = 0.08$), in agreement to the common easiness with which dynamical analyses are performed from variable x of the Rössler system. Contrary to this, the manifold observability coefficient $\eta_z^{\mathcal{M}}$ is quite small ($\eta_z^{\mathcal{M}} = 0.10$ with $P_{\mathcal{M}_z^{\rm obs}} = 0.22$ and $\overline{T}_{\mathcal{M}_z^{\rm obs}} = 0.88$) (Fig. 2b) due to the long time spent in $\mathcal{U}_{\mathcal{M}_z^{\rm obs}}$. As a consequence, the lack of observability induced by variable z of the Rössler system is stronger and much more influent than the lack of observability induced by variable x. The coefficient $\eta_x^{\mathcal{M}}$ strongly depends on ϵ as reported in Tab. I. Obviously the thickness ϵ increases the coefficient $P_{\mathcal{M}_x^{\rm obs}}$ and, thus, decreases $\eta_x^{\mathcal{M}}$. Since the dependency starts to be damped around $\mu = 0.05$, we will retain ϵ corresponding to $\mu = 0.05$ for our analyses.

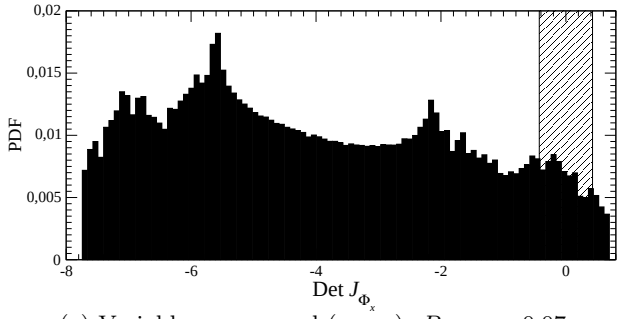

(a) Variable x measured ($s = x$): $P_{\mathcal{M}_x^{\rm obs}} = 0.07$

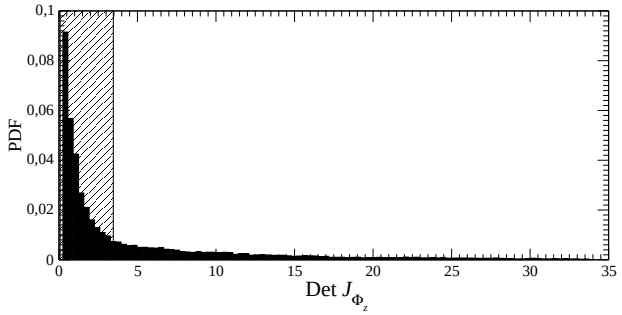

(b) Variable z measured ($s = z$): $P_{\mathcal{M}_z^{\rm obs}} = 0.22$

FIG. 2: Probability density function of Det $\mathcal{J}_{\Phi_x}$ and Det $\mathcal{J}_{\Phi_z}$ for a typical trajectory on the chaotic attractor solution to the Rössler system (8). The neighborhoods $\mathcal{U}_{\mathcal{M}_s^{\rm obs}}$ are represented as hatched domain. Parameter values: $a = 0.398$, $b = 2$ and $c = 4$.

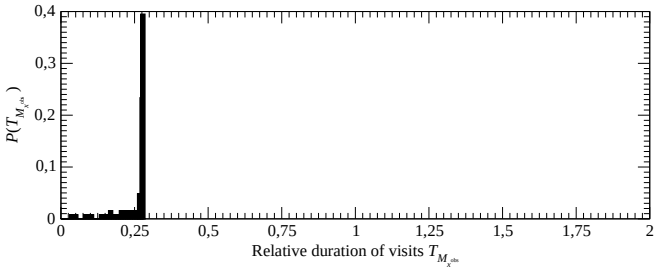

(a) Case of $\mathcal{M}_x^{\rm obs}$

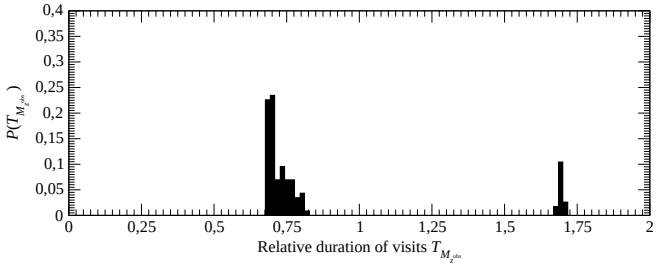

(b) Case of $\mathcal{M}_z^{\rm obs}$

FIG. 3: Probability of duration for visiting the neighborhood of singular observability manifold $\mathcal{M}_s^{\rm obs}$. Case of the Rössler system (8). Parameter values: $a = 0.398$, $b = 2$, and $c = 4$.

TABLE I: Manifold observability coefficient $\eta_s^{\mathcal{M}}$ for the variables not inducing a full observability. Case of the Rössler system ($a = 0.398$, $b = 2$ and $c = 4$) and the Lorenz system ($R = 28$, $\sigma = 10$ and $b = 8/3$).

	Rössler		Lorenz		
μ	$\eta_x^{\mathcal{M}}$	$\eta_z^{\mathcal{M}}$	$\eta_x^{\mathcal{M}}$	$\eta_y^{\mathcal{M}}$	$\eta_z^{\mathcal{M}}$
0.005	0.99	0.45	0.94	0.73	0.62
0.010	0.97	0.45	0.88	0.60	0.48
0.020	0.94	0.33	0.78	0.34	0.41
0.030	0.91	0.26	0.70	0.21	0.35
0.040	0.89	0.15	0.63	0.13	0.31
0.050	0.86	0.10	0.57	0.10	0.28

C. Case of the Lorenz system

Let us now consider the Lorenz system [20]. The determinants of the jacobian matrices associated with the three different coordinate transformations Φ_s (with $s = x$, y, z) are

$$\begin{cases} \mathcal{J}_{\Phi_x} = -\sigma^2 x \\ \mathcal{J}_{\Phi_x} = R(\sigma y - bx) - \sigma yz + 2x^2 y \\ \mathcal{J}_{\Phi_x} = 2\sigma y^2 + 2x^2(z - R)\,, \end{cases} \tag{19}$$

respectively. The corresponding probability density functions are shown in Fig. 4. The neighborhood $\mathcal{U}_{\mathcal{M}_x^{\rm obs}}$ is less often visited than the neighborhood $\mathcal{U}_{\mathcal{M}_y^{\rm obs}}$, meaning thus that the lack of observability of the Lorenz dynamics will be less influent when variable x ($P_{\mathcal{M}_x^{\rm obs}} = 0.19$) is measured than when variable y ($P_{\mathcal{M}_y^{\rm obs}} = 0.69$) is measured. The case of variable z ($P_{\mathcal{M}_z^{\rm obs}} = 0.40$) corresponds to an intermediate case. This means that the analyses would be better from variable z than from variable y, excepted that all information about the symmetry would be lost in the former case.

The singular observability manifolds $\mathcal{M}_s^{\rm obs}$ defined by

$$\begin{cases} \mathcal{M}_x^{\rm obs} = \left\{(x,y,z) \in \mathbb{R}^3 \mid -\sigma^2 x = 0\right\} \\ \mathcal{M}_y^{\rm obs} = \left\{(x,y,z) \in \mathbb{R}^3 \mid z = R - \frac{Rbx}{\sigma y} + \frac{2x^2}{\sigma}\right\} \\ \mathcal{M}_z^{\rm obs} = \left\{(x,y,z) \in \mathbb{R}^3 \mid z = R - \sigma\left(\frac{y}{x}\right)^2\right\} \end{cases} \tag{20}$$

are quite complicated as shown in Fig. 5. From these figures, it clearly appears that $\mathcal{M}_x^{\rm obs}$ is almost perpendicular to the vector field $\boldsymbol{f}$ defined by the Lorenz system (9) and has therefore a low influence on the reconstruction procedure (Fig. 5a). $\mathcal{M}_y^{\rm obs}$ and $\mathcal{M}_z^{\rm obs}$ are both complicated and intersects in different places the Lorenz attractor $\mathcal{A}$ (Figs. 5b and 5c). The probabilities with which the neighborhood $\mathcal{U}_{\mathcal{M}_s^{\rm obs}}$ are visited are reported in Tab. II with the relative time spent in it. The manifold observability coefficient ($\eta_x^{\mathcal{M}} = 0.57$) for variable x is nearly twice the coefficient for variable z ($\eta_z^{\mathcal{M}} = 0.28$), thus confirming what is commonly observed, that is, it is easier to get a global model from variable x than from variable z. Our coefficients $\eta_s^{\mathcal{M}}$ thus explain well the observability coefficients obtained and why variable x is definitely the best variable for investigating the Lorenz dynamics. These manifold observability coefficients also explain why the Lorenz dynamics is rather more difficult to reliably investigate than the Rössler dynamics investigated from variable y or from variable x.

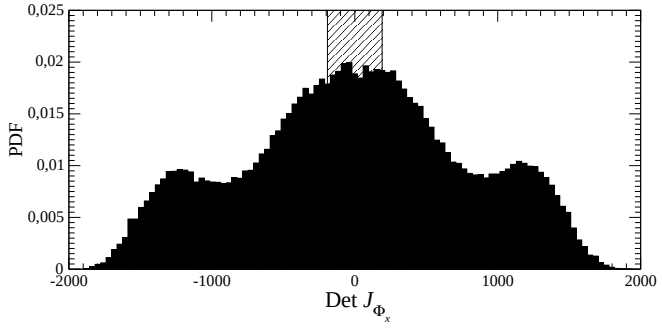

(a) Variable x measured ($s = x$)

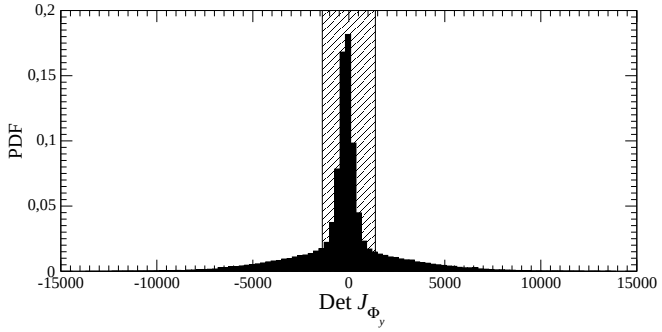

(b) Variable y measured ($s = y$)

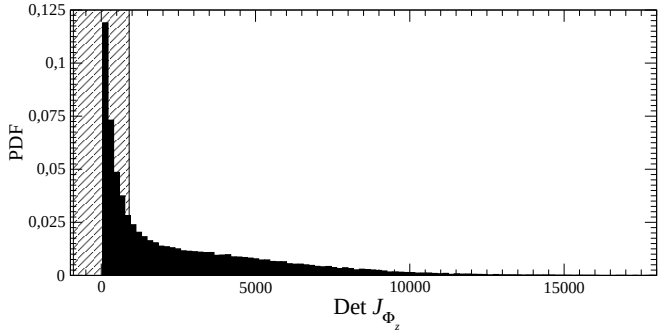

(c) Variable z measured ($s = z$)

FIG. 4: Probability density function of Det $\mathcal{J}_{\Phi_s}$ (with $s = x$, y, and z) for a typical trajectory on the chaotic attractor solution to the Lorenz system (9). The neighborhoods $\mathcal{U}_{\mathcal{M}_s^{\rm obs}}$ are represented as hatched domain. Parameter values: Parameter values: $R = 28$, $\sigma = 10$ and $b = 8/3$.

TABLE II: Probability of visits of the singular observability manifolds $\mathcal{M}_s^{\text{obs}}$, the time spent in the corresponding neighorhoods and the manifold observability coefficients $\eta_s^{\mathcal{M}}$ for the Rössler and the Lorenz systems.

	s	$P_{\mathcal{M}_s^{\text{obs}}}$	$\overline{T}_{\mathcal{M}_s^{\text{obs}}}$	$\eta_s^{\mathcal{M}}$
Rössler system	x	0.07	0.08	0.86
	z	0.22	0.88	0.10
Lorenz system	x	0.19	0.30	0.57
	y	0.69	0.69	0.10
	z	0.31	0.59	0.28

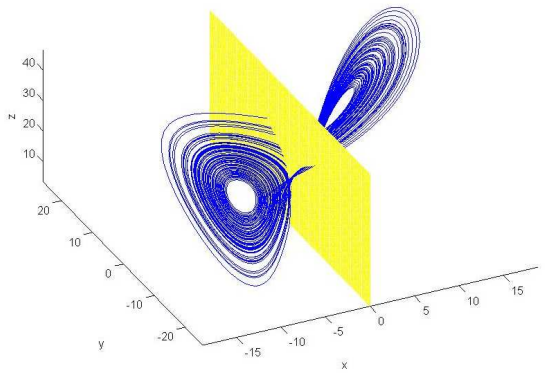

(a) Variable x measured ($s = x$)

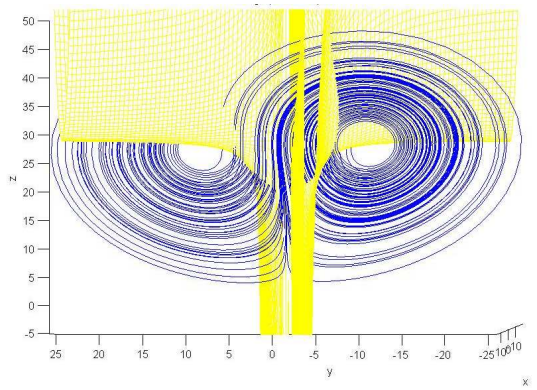

(b) Variable y measured ($s = y$)

FIG. 5: Chaotic attractor solution to the Lorenz system (9) and the singular observability manifolds $\mathcal{M}_s^{\text{obs}}$ for each of the variables. Parameter values: $R = 28$, $\sigma = 10$, and $b = 8/3$.

IV. SINGULAR OBSERVABILITY MANIFOLD AND SYNCHRONIZATION

The interplay between observability and synchronization was recently shown for bidirectional coupling between two nearly identical systems [18]: the range of values of the coupling parameter for which complete and/or phase synchronization can be obtained is the largest when the systems are coupled *via* a variable providing a good observability as shown, for instance, in the case of two Rössler systems bidirectionaly coupled

$$\begin{cases} \dot{x}_{1,2} = \omega_{1,2}\left[-y_{1,2} - z_{1,2}\right] + \rho_x(x_{2,1} - x_{1,2}) \\ \dot{y}_{1,2} = \omega_{1,2}\left[x_{1,2} + a y_{1,2}\right] + \rho_y(y_{2,1} - y_{1,2}) \\ \dot{z}_{1,2} = \omega_{1,2}\left[b + z_{1,2}(x_{1,2} - c)\right] + \rho_z(z_{2,1} - z_{1,2}), \end{cases} \tag{21}$$

where $\delta\omega = \omega_1 - \omega_2 = 0.04$ is a slight detuning between the two Rössler systems (Fig. 6).

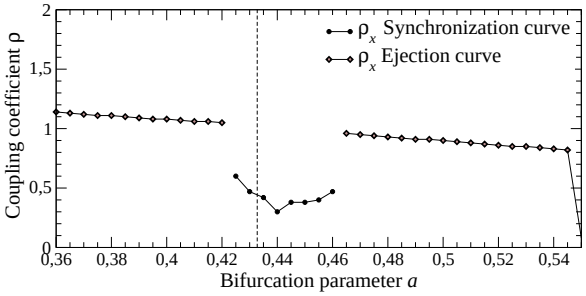

FIG. 6: Critical coupling curves that correspond to the onset of synchronization (synchronization curve) and the ejection of the trajectory to infinity (ejection curve), respectively. Below the synchronization curve, the average distance between points and the first bisecting line of plane y_1-y_2 is greater than 0.1. Case of the Rössler system, $b = 2$, $c = 4$ and $\delta\omega = 0.04$.

By increasing the value of parameter a from 0.36 (first limit cycle of the period-doubling cascade) to 0.555 (just before the ejection to infinity that occurs), we observed that the synchronizability between two non-identical Rössler systems depends on the dynamical regime. For the largest a-values, the attractor boundary was very close to the boundary of the attraction basin and it was nearly impossible to get a synchronization without provoking an ejection to infinity as shown by the ejection curve when the two systems are coupled with variable x. For this reason, in the case of variable x, two critical curves were plotted: i) if complete synchronization occurs, we showed the ("synchronization curve") lowest value of the coupling terms ρ_0 for which this happens. On the other hand, ii) if complete synchronization did *not* happen, we show the ("ejection curve") coupling strength ρ_∞ at which the trajectory was ejected to infinity. This means that, for the particular value of the bifurcation parameter, if $\rho_x < \rho_\infty$ the coupled system is stable but is *not* synchronized, and if $\rho_x \geq \rho_\infty$ the coupled system becomes unstable.

When variable x was used to couple the two non-identical Rössler systems, complete synchronization was only obtained over the range $a \in [0.425; 0.455]$ (Fig. 6). By computing the evolution of the probability of visits $P_{\mathcal{M}_x^{\text{obs}}}$ versus parameter a, it is remarked that this range corresponds to the parameter range for which the probability $P_{\mathcal{M}_x^{\text{obs}}}$ is minimal. Such a feature thus connect

the probability of visits of the neighborhood $\mathcal{U}_{\mathcal{M}_x^{\rm obs}}$ with the synchronizability. There is no change in the algebraic structure of the Rössler system when parameter a is varied. Contrary to this, there is a direct influence of a-value on $P_{\mathcal{M}_x^{\rm obs}}$ which is sufficient to explain why complete synchronization is observed in that particular range (Fig. 7). With the help of the probability of visits of the neighborhood $\mathcal{U}_{\mathcal{M}_x^{\rm obs}}$, we were thus able to confirm the origin of the dynamical contribution to synchronizability mentioned in [18], that is, the role played by the singular observability manifold.

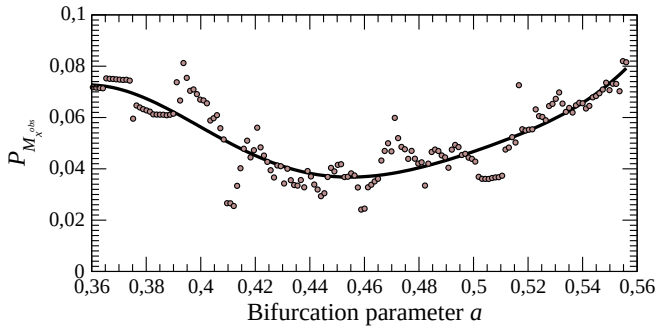

FIG. 7: Evolution of the probability of visits of the singular observability manifold $\mathcal{M}_x^{\rm obs}$ versus parameter a of the Rössler system. Other parameter values: $b = 2$ and $c = 4$.

It must be remarked that the probability $P_{\mathcal{M}_x^{\rm obs}}$ does not evolve continuously when parameter a is varied (Fig. 7). This results from the fact that the probability of visits of a Poincaré section of the attractor is not a smooth curve but a rather peaked function, the peaks corresponding to the neighborhood of the periodic points of the last created periodic orbits. Such a probability of visits does not therefore vary in a continuous way when a bifurcation parameter is varied, since it is very sensitive to the orbit involved in the last bifurcation. The last created orbit is the most often visited (see [24] for instance). This is why we fitted a 8th order polynomial to the computed probabilities to exhibit the mean tendency (Fig. 7). Moreover, the relative time $\overline{T}_{\mathcal{M}_x^{\rm obs}}$ spent in the neighborhood $\mathcal{U}_{\mathcal{M}_x^{\rm obs}}$ decreases to 0.05 when a is set to 0.43295, thus contributing to our ability to obtain a complete synchronization using variable x.

V. CONCLUSION

Observability coefficients are useful measures to explain why better results are obtained when a dynamical system is investigated from a given variable rather than from another one. They were thus used to rank the variables of a system according to the observability of the attractor they provide. Unfortunately, these coefficients are not normalized and do not allow to compare the variables of a system with those of another system. The symbolic coefficients were thus introduced but they only take into account the algebraic structure of the system considered. In other words, they do not consider the relative organization of the attractor and the singular observability manifold as implicitely considered by the numerical observability coefficients initially introduced. To overcome this difficulty, we introduced two measures easily computed, the probability of visits of the singular observability manifold and the relative time spent in its neighborhood were introduced. We showed that it was thus possible to introduce a manifold observability coefficient which quantifies the contribution of the dynamical regime to the observability coefficients, the algebraic contribution being provided by the symbolic observability coefficients. Two ingredients were used to build these coefficients, the location of the singular observability manifold $\mathcal{M}_s^{\rm obs}$ with respect to the attractor and the relative time in the neighborhood of this manifold.

It is therefore now possible to possess normalized coefficients which allow to compare variables from various systems; something which is still not possible to do with the numerical observability coefficients. Moreover, our two measures distinguish accurately what is the origin of the influence of the observability defects on any dynamical analysis. Note that building observability coefficients taking into account symmetry properties as observed in the Lorenz system is still an open problem since none of the coefficients nor the measures introduced in this paper take into account this aspect of the problem.

[1] F. Takens, Detecting strange attractors in turbulence, *Lecture Notes in Mathematics*, **898**, 366-381, 1981.

[2] D. Aeyels, Generic observability of differentiable systems, *SIAM Journal of Control and Optimization*, **19** (5), 595-603, 1981.

[3] G. Gouesbet & C. Letellier, Global vector field reconstruction by using a multivariate polynomial L_2-approximation on nets, *Physical Review E*, **49** (6), 4955-4972, 1994.

[4] L. A. Aguirre. Controllability and observability of linear systems: some noninvariant aspects, *IEEE Transactions on Education*, **38**, 33-39, 1995.

[5] C. Letellier & L. A. Aguirre, Investigating nonlinear dynamics from time series: the influence of symmetries and the choice of observables, *Chaos*, **12**, 549-558, 2002.

[6] C. Letellier, L. A. Aguirre & J. Maquet, Relation between observability and differential embeddings for nonlinear dynamics, *Physical Review E*, **71**, 066213, 2005.

[7] C. Letellier, L. A. Aguirre & J. Maquet, How the choice of the observable may influence the analysis of nonlinear dynamical system, *Communications in Nonlinear*

Science and Numerical Simulation, **11**, 555-576, 2006.

[8] C. Letellier & L. A. Aguirre, Graphical interpretation of observability in terms of feedback circuits, *Physical Review E*, **72** (5), 056202, 2005.

[9] G. P. King & I. Stewart, Phase space reconstruction for symmetric dynamical systems, *Physica D,* **58**, 216-228, 1992.

[10] T. Kailath. *Linear Systems*, Englewood Cliffs, NJ, Prentice Hall, 1980.

[11] C. T. Chen, *Linear Systems Theory and Design*, 3rd Edition, Oxford University Press, 1999.

[12] R. Hermann & A. Krener, Nonlinear controllability and observability, **22** (5), 728–740, 1977.

[13] W. Perruquetti & J-P. Barbot, *Chaos in automatic control*, CRC Press, 2006.

[14] L. Cao, A. Mees & K. Judd, Dynamics from multivariate time series, *Physica D*, **121**, 75-88, 1998.

[15] A. J. Krener & W. Respondek, A nonlinear observer with linearizable error dynamics, *SIAM Journal on Control and Optimization*, **23**, 197–216, 1985.

[16] X. H. Xia & W. B. Gao, Nonlinear observer design by observer error linearization, *SIAM Journal on Control and Optimization*, **27**, 199–216, 1989.

[17] T. Boukhobza, M. Djemai & J.-P. Barbot, Implicit triangular observer form dedicated to a sliding mode observer for systems with unknown inputs, *Asian Journal of Control*, **5** (4), 513–527, 2003.

[18] C. Letellier & L. A. Aguirre, Interplay between synchronization, observability, and dynamics, *Physical Review E*, **82** (1), 016204, 2010.

[19] O. E. Rössler, An equation for continuous chaos, *Physics Letters A*, **57** (5), 397-398, 1976.

[20] E. N. Lorenz, Deterministic nonperiodic flow, *Journal of the Atmospheric Sciences,* **20**, 130-141, 1963.

[21] M. Ghanes, J. De Leon & A. Glumineau, Cascade and high-gain observers comparison for sensorless closed-loop induction motor control, *IET Control Theory and Applications*, **2** (2), 133-150, 2008.

[22] M. Ghanes, J.-P. Barbot, J. DeLeon & A. Glumineau, A robust output feedback controller of the induction motor drives: new design and experimental validation, *International Journal of Control*, **83**, 484-497, 2010.

[23] J. D. Farmer, J. P. Crutchfield, H. Frœling, N. H. Packard & R. S. Shaw, Power spectra and mixing properties of strange attractors, *Annals of the New York Academy of Sciences*, **357**, 453-472, 1980.

[24] Hao Bai Lin, *Elementary symbolic dynamics and chaos in dissipative systems*, World Scientific Publishing, Singapore, 1989.